Progress In Electromagnetics Research Letters, Vol. 109, 111–117, 2023

A Miniaturized Band-Stop FSS Based on Pixelated Unitcell

Abedin Karimi and Morteza Nadi*

Abstract—As wireless devices become increasingly compact, portable, and accessible anywhere, there is a need to increase isolation between them and reduce frequency interference. The purpose of this paper is to suppress interference by using pixelated patterns on a single layer in a miniaturized unitcell. To miniaturize of unitcell, the surface was pixelated into 50×50 pixels with a resolution of $0.2\,\text{mm} \times 0.2\,\text{mm}$. The proposed unitcell occupies a small area of $0.06\lambda_0 \times 0.06\lambda_0$ at GSM frequency ($f = 1.8\,\text{GHz}$). The pixelation of the surface allows the surface current to follow a long path. Therefore, unlike the previous works, the miniaturized structure is obtained using a 1D layer without any vias and lumped elements. A significant advantage of this structure is that it is significantly more miniaturized than the current state-of-the-art unitcells and allows for a wider range of applications. Full-wave simulation and measurement results are in good agreement with each other and show stopband at operation frequency. As a result, both simulation and measurement results show that the proposed structure has a dual-polarized characteristic with good angular stability under a variety of incidence angles.

1. INTRODUCTION

Over the past decades, metasurfaces, or 2D-dimensional metamaterials, have attracted significant attention from researchers due to their ability to modify permittivity and permeability beyond natural material composites. Metasurfaces have been extensively used in various microwave applications, such as metasurface antenna [1–3], radar cross-section (RCS) reduction [4], reflectarray antenna [5], electromagnetic shielding enclosure [6], and spatial filters [7–22]. Typically, metasurfaces consist of scattering arrays of metallic patches exhibiting one or more passbands or stopbands.

Recently, multi-frequency systems and multiple input-multiple output (MIMO) systems have been studied widely in order to improve the quality of wireless communication and satisfy users. If there is a small frequency interval between two operating bands, interference suppuration increases for multiple antenna systems. A spatial filter such as a frequency selective surface (FSS) can suppress interference on a particular frequency range.

Traditional spatial filters are constructed by periodic metallic patches and slot arrays that are placed on dielectric layers. There is low cost and easy manufacturing associated with these planar structures. A unitcell can be designed using a number of parameters, including dimension, shape, dielectric permittivity, number of layers, thickness, etc., to achieve similar performance at different oblique incident angles, whether transverse electric (TE) or transverse magnetic (TM). Several types of research have proposed different configurations of unitcells to develop a high-performance spatial filter. For instance, [7] proposes a new reconfigurable four-arms star frequency selective surface by appropriately embedding PIN diode to realize reconfigurable FSS with two distinct resonance frequencies. In [8], a new analytical method is introduced based on equivalent circuits of square and hexagonal patches for designing a first-order bandpass FSS. In another study, [9], an angular independent higher order band-stop frequency was designed using curved arms of a conventional cross dipole. The structure

Received 24 December 2022, Accepted 28 February 2023, Scheduled 22 March 2023
* Corresponding author: Morteza Nadi (m_nadi@elec.iust.ac.ir).
The authors are with the Iran University of Science and Technology, Iran.

in [10] was implemented using via holes and multilayer printed circuits board substrate to proposed 3D-FSS. A novel FSS with quasi-elliptical bandpass filtering response is proposed in [11] with hollow metal pipe arrays and metal disk arrays printed on thin substrate layers. There is a flat transmission in the passband and a fast roll-off in this structure. A new structure for switching from bandstop to bandpass operation is proposed in [12] without the requirement to integrate active devices. This structure is composed of helical resonators that can adjust the height of a mechanical spring in order to tune the frequency of resonance and switch between bandstop and bandpass modes [13], and the authors used supervised machine learning (ML) with the decision tree (DT) algorithm to synthesize multiband frequency selective surfaces (FSSs). In [14] unlike the traditional FSSs, which make use of a resonant metallic or slot structure, bandpass is made up of metallic patches separated by thin air-gaps backed by a wire mesh.

Many efforts have been made to achieve miniaturization of unitcell, which is often required at lower frequencies. The miniaturized unitcell is achieved by the fractal elements, vertical holes, multilayer structures, etc. A miniaturized bandpass FSS based on a fractal array is presented in [15]. To minimize the size of unitcells, the authors used the Minkowski island-shaped patches which exhibit a lower frequency against profile than conventional FSSs. In [16], instead of a 2D planar FSS, a miniaturized dual-band and dual-polarized bandpass FSS was proposed by adding vertical metalized holes (vias) to the substrate which act as additional capacitive elements. In [17], The miniaturized two-band band-stop filter was obtained by a 2.5D structure composed of a meandering-line connecting vertical via arrays on a dielectric layer.An approach to further miniaturizing convoluted bandpass FSS unitcells involves loading capacitive structures is proposed in [18]. In this approach, convoluted bandpass elements are cascaded with convoluted slot grids (CSGs), which function as parallel LC circuits and parallel capacitors, reducing the size of unitcells. Another miniaturized FSS is proposed in [19], and the dual stopband characteristic is achieved by printing meander lines on a single-layer dielectric substrate. A miniaturized dual-band FSS with anchor-shaped loops for WLAN frequency was presented in [20].

This paper proposes miniaturized element frequency selective surfaces (MEFSSs) with band-reject characteristics for both transverse electric (TE) and transverse magnetic (TM) polarizations. The surface was pixelated into 50×50 pixels with a resolution of $0.2\,\text{mm} \times 0.2\,\text{mm}$ to achieve high miniaturization at lower frequencies under normal and oblique incidents with both TE and TM polarizations. The performance of the proposed spatial filter is demonstrated under normal and oblique incidences with full-wave simulations and measurements. In addition, the proposed spatial filter is more compact than previously published ones.

2. DESIGN AND SIMULATION

FSS band-reject is fundamentally based on LC resonance, implying that the resonance frequency and resonator length can be determined analytically by [21]. The proposed structure is symmetrical with regard to the normal axis of unitcell in order to reduce the sensitivity of this structure to the polarization of the incident wave. Hence, the equivalent circuits of the structure are the same for both the vertical and horizontal polarizations. The stopband filter is obtained by the LC series network, in which the capacitance and inductance of the unitcell can determine the resonant frequency of this network. Our goal is to minimize the dimension of the unitcell for a desired resonance frequency by adjusting the capacitance and inductance values of the unitcell. In general, the effective capacitance of a unitcell can be approximated by the following closed-form expression [21].

$$C = \frac{2p\varepsilon_0\varepsilon_r}{\pi} Ln\left(\frac{1}{\sin\left(\frac{\pi s}{2p}\right)}\right) \tag{1}$$

where p is the period of unitcell, s the gap between two adjacent patches, and h the dielectric constant of the medium that the resonator layer is printed on. However, the inductance value is only determined by the length and width of the metallic strip, p and w [21].

$$L = \frac{\mu_0 p}{2\pi} Ln\left(\frac{1}{\sin\left(\frac{\pi w}{2p}\right)}\right) \tag{2}$$

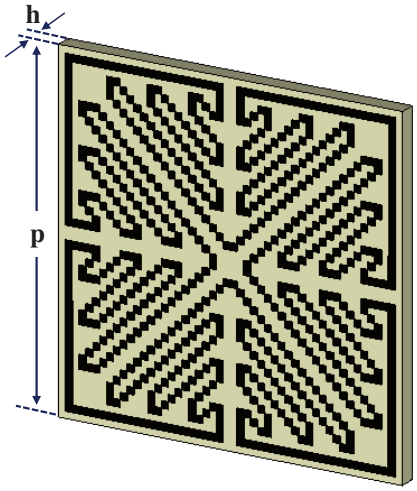

Figure 1. Schematic of proposed pixelated unitcell.

Therefore, our approach in this paper is to miniaturize the unitcell against wavelength. For this purpose, the surface of the symmetric unitcell was pixelated into 50×50 pixels with a resolution of $0.2\,\text{mm} \times 0.2\,\text{mm}$, as shown in Fig. 1. It is worth noting that, unlike the previous works, the proposed structure is 1D and has a simple design. It should be noted that the proposed FSS is implemented on an FR-4 laminated substrate with a dielectric constant of 4.4, a loss tangent of 0.027, and a thickness of $h = 0.5\,\text{mm}$. Its geometry is shown in Fig. 1, where the periodicity of the unitcell is $p = 10\,\text{mm}$, while the wavelength of the resonance frequency is 166 mm. Thus, the terms of the figure-of-merit (λ_0/p) are around 16. In fact, the resonant frequency of the FSS would become lower because the total conductor length is three times longer than the planar square loop; the conventional band-stop spatial filters are on the same substrate when the thickness is 0.5 mm.

The transmission and reflection coefficients of the proposed structure are shown in Fig. 2. The commercial software CST Microwave Studio is employed, where periodic boundary conditions are applied along with the lateral directions, while Floquet ports are assigned to the z-direction. As observed from the simulation results obtained, Fig. 2, the resonance frequency of this structure located at 1800 MHz in contrast to the resonance frequency of the planar square loop is 4430 MHz at the same condition.

A variation in substrate thickness will change the resonance frequency of the FSS since the thickness

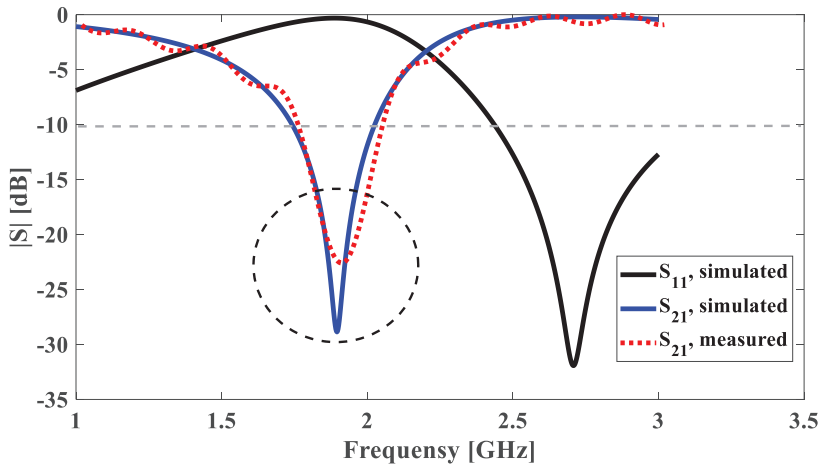

Figure 2. Reflection and transmission coefficients of the proposed pixelated unitcell.

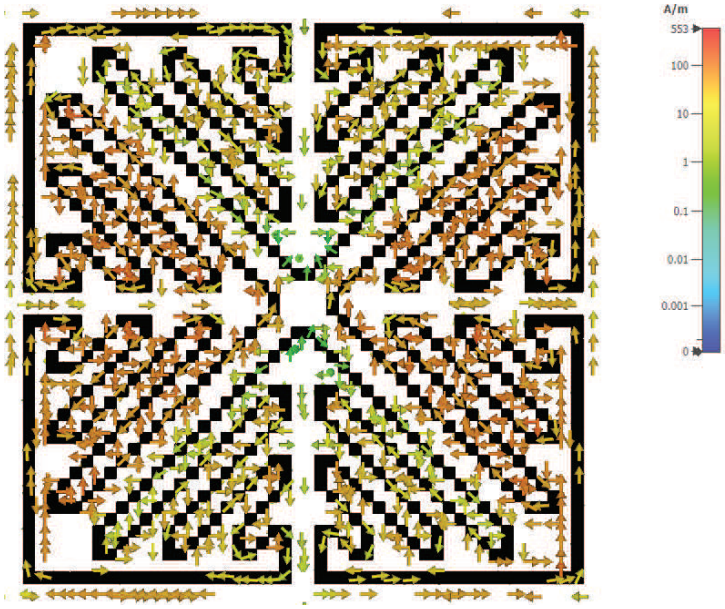

Figure 3. The surface current distribution of the band stop structure at $f = 1.8\,\text{GHz}$.

will affect the capacitance of unitcell. Due to this fact, the thickness of the substrate is set to 0.5 mm to study only the behavior of metal layer and reduce the effect of substrate on resonance frequency.

Figure 3 illustrates the resonance mechanism of the pixelated unitcell by showing the surface current distribution under normal incident waves. This figure indicates that the pixelation of the surface allows a long path to be selected for the surface current pass. Fig. 4 depicts the frequency response of the proposed structure in different oblique incident angles at both TE and TM polarizations up to 80°, respectively. It can be observed that the resonant frequency is quite stable up to 50°. the bandwidth of resonance becomes wider for TE mode with increasing the incident angle while it tends to decrease in the TM mode. In addition, the simulation and measurement results exhibit that the FSS offers almost total reflection at the resonant frequencies.

For the real-world application, the proposed structure with 20×20 elements was fabricated on an FR-4 substrate, as shown in Fig. 5(a), by using standard printing board (PCB) process technology. Structural parameters of the fabricated structure are the same as the simulated ones mentioned above. A free-space measuring system is used for measuring the transmission coefficients of the fabricated FSS, as shown in Fig. 5(b). Regarding Fig. 5(b), the measurement setup is mainly composed of transmitting and receiving standard-gain horn antennas, and a frame that was covered by electromagnetic absorber material to reduce reflected rays back to the antennas and a vector network analyzer. The fabricated FSS structure is placed on the center of the frame and in the middle of transmitting and receiving antennas with a distance of 3 m and 0.5 m, respectively. To ensure measurement accuracy, transmission coefficients were measured without the FSS prototype. The transmission coefficients of the FSS prototype were calibrated based on these measured results.

The measured transmission coefficient of the fabricated structure under a normal incident wave is shown in Fig. 2. It can be observed that full-wave simulation and measurement results are in good agreement with each other. As expected, the proposed structure has a stopband frequency at the GSM band ($f = 1.8\,\text{GHz}$). There are slight discrepancies between the simulation and measurement results, including unexpected ripples in the measured transmission curves. The unexpected ripples in the experimental data could be attributed to the errors in the measuring system, such as the edge diffraction of the fabricated structure.

Table 1 shows the comparison between the proposed FSS structure and the structures reported previously; the table shows the advantage of specification rather than the other references. In more detail, the proposed structure has more miniaturized dimension than the previous works. Moreover, this structure exhibits a band-stop spatial filter by using a simple and low-cost structure.

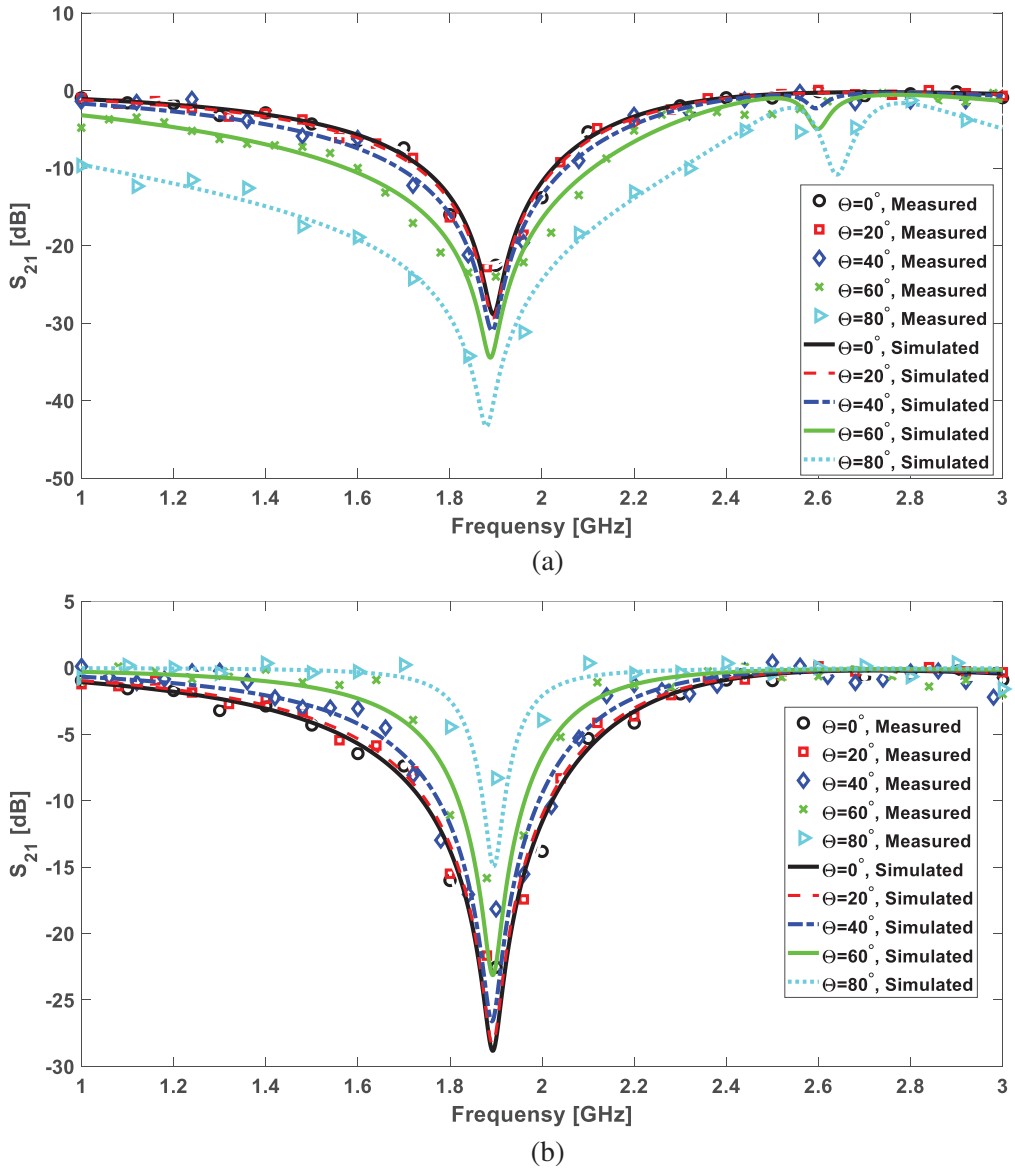

Figure 4. Simulated and measured transmission coefficient at different incidence angles for (a) TE polarization, (b) TM polarization.

Table 1. Comparison of the proposed miniaturize unitcell with state of the art references.

Refrence	Metal layer	Resonant frequency (GHz)	Uintcell size $\lambda_0 \times \lambda_0$	Substrate thickness (mm)
Ref. [16]	1-layer, 2.5D	2.4, 5	0.067×0.067	FR-4, 1.6
Ref. [17]	1-layer, 2.5D	2.4, 5	0.05×0.05	FR-4, 1.6
Ref. [20]	1-layer, 2D	2.4, 5	0.65×0.65	FRB-2, 1.5
Ref. [22]	1-layer, 2.5D	2.1	0.064×0.064	FR-4, 1.6
This Study	1-layer, 2D	1.8	0.06×0.06	FR-4, 0.5

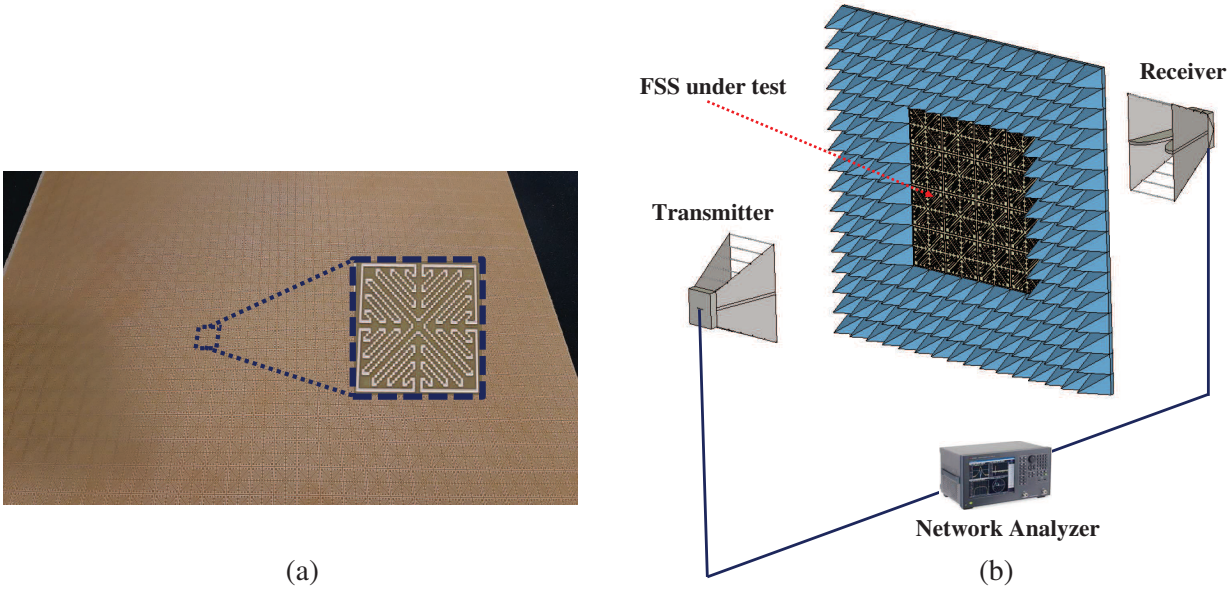

Figure 5. (a) Fabricated prototype of the pixelated band-stop FSS. (b) Measurement setup.

3. CONCLUSION

In summary, this paper proposes a miniaturized unitcell for a stopband spatial filter. In this method, the surface of the unitcell is pixelated to create a long path for the surface current to pass. The total conductor of this structure is three times longer than the planar square loop at the same frequency band. Therefore, unlike the previous works, the miniaturized structure is obtained using a 1D layer without any lumped element. Moreover, the proposed structure provides the stable frequency response at different oblique incident angles in both TE and TM polarizations up to 50°, respectively. As a proof of a concept, the proposed structure with 20×20 elements was fabricated on an FR-4 substrate and tested. The measurement result corroborated well with full-wave simulation at operation frequency.

REFERENCES

1. Faenzi, M., G. Minatti, D. González-Ovejero, F. Caminita, E. Martini, C. D. Giovampaola, and S. Maci, "Metasurface antennas: New models, applications and realizations," *Scientific Reports*, Vol. 9, No. 1, 1–14, 2019.
2. Nadi, M., H. Rajabalipanah, A. Cheldavi, and A. Abdolali, "Flexible manipulation of emitting beams using single-aperture circularly polarized digital metasurface antennas: Multibeam radiation toward vortex-beam generation," *Advanced Theory and Simulations*, Vol. 3, No. 4, 1900225, 2020.
3. Rajabalipanah, H., M. Nadi, A. Abdolali, and A. Cheldavi, "Highly efficient metaradiators with circular polarization," *Journal of Applied Physics*, Vol. 128, No. 11, 114503, 2020.
4. Nadi, M., S. H. Sedighy, and M. Khalaj-Amirhosseini, "Ultra wideband radar cross section reduction by using non-resonant unit cells," *Scientific Reports*, Vol. 10, No. 1, 1–10, 2020.
5. Khalaj-Amirhosseini, M. and M. Nadi-Abiz, "Reducing the sidelobe level of reflectarray antennas using phase perturbation method," *Iranian Journal of Electrical and Electronic Engineering*, Vol. 16, No. 2, 153–157, 2020.
6. Hashemi, S. and A. Abdolali, "Room shielding with frequency-selective surfaces for electromagnetic health application," *International Journal of Microwave and Wireless Technologies*, Vol. 9, No. 2, 291–298, 2017.

7. Mamedes, D. F., A. G. Neto, J. C. e Silva, and J. Bornemann, "Design of reconfigurable frequency-selective surfaces including the pin diode threshold region," *IET Microwaves, Antennas & Propagation*, Vol. 12, No. 9, 1483–1486, 2018.
8. Fallah, M. and M. H. Vadjed-Samiei, "Designing a bandpass frequency selective surface based on an analytical approach using hexagonal patch-strip unit cell," *Electromagnetics*, Vol. 35, No. 1, 25–39, 2015.
9. Kocakaya, A. and G. Çakır, "Novel angular-independent higher order band-stop frequency selective surface for X-band applications," *IET Microwaves, Antennas & Propagation*, Vol. 12, No. 1, 15–22, 2018.
10. Lee, I. G. and I. P. Hong, "3D frequency selective surface for stable angle of incidence," *Electronics Letters*, Vol. 50, No. 6, 423–424, 2014.
11. Zhao, Z., A. Zhang, X. Chen, G. Peng, J. Li, H. Shi, and A. A. Kishk, "Bandpass FSS with zeros adjustable quasi-elliptic response," *IEEE Antennas and Wireless Propagation Letters*, Vol. 18, No. 6, 1184–1188, 2019.
12. Azemi, S. N., K. Ghorbani, and W. S. T. Rowe, "A reconfigurable FSS using a spring resonator element," *IEEE Antennas and Wireless Propagation Letters*, Vol. 12, 781–784, 2013.
13. Fontoura, L. C. M. M., H. W. De Castro Lins, A. S. Bertuleza, A. G. Dassunção, and A. G. Neto, "Synthesis of multiband frequency selective surfaces using machine learning with the decision tree algorithm," *IEEE Access*, Vol. 9, 85785–85794, 2021.
14. Sarabandi, K. and N. Behdad, "A frequency selective surface with miniaturized elements," *IEEE Transactions on Antennas and Propagation*, Vol. 55, No. 5, 1239–1245, 2007.
15. Zheng, S., Y. Yin, J. Fan, X. Yang, B. Li, and W. Liu, "Analysis of miniature frequency selective surfaces based on fractal antenna-filter-antenna arrays," *IEEE Antennas and Wireless Propagation Letters*, Vol. 11, 240–243, 2012.
16. Yeganeh, A. N., S. Mohammad-Ali-Nezhad, S. H. Najmolhoda, and S. H. Sedighy, "Dual-band, dual-polarized, and compact frequency selective surface," *International Journal of RF and Microwave Computer-Aided Engineering*, Vol. 29, No. 9, e21810, 2019.
17. Wei, P.-S., C.-N. Chiu, and T.-L. Wu, "Design and analysis of an ultraminiaturized frequency selective surface with two arbitrary stopbands," *IEEE Transactions on Electromagnetic Compatibility*, Vol. 61, No. 5, 1447–1456, 2018.
18. Zhao, P.-C., Z.-Y. Zong, W. Wu, B. Li, and D.-G. Fang, "Miniaturized-element bandpass FSS by loading capacitive structures," *IEEE Transactions on Antennas and Propagation*, 67, No. 5, 3539–3544, 2019.
19. Ghosh, S. and K. V. Srivastava, "An angularly stable dual-band FSS with closely spaced resonances using miniaturized unit cell," *IEEE Microwave and Wireless Components Letters*, Vol. 27, No. 3, 218–220, 2017.
20. Yan, M., S. Qu, J. Wang, J. Zhang, H. Zhou, H. Chen, and L. Zheng, "A miniaturized dual-band FSS with stable resonance frequencies of 2.4 GHz/5 GHz for WLAN applications," *IEEE Antennas and Wireless Propagation Letters*, Vol. 13, 895–898, 2014.
21. Al-Joumayly, M. A. and N. Behdad, "A generalized method for synthesizing low-profile, bandpass frequency selective surfaces with non-resonant constituting elements," *IEEE Transactions on Antennas and Propagation*, Vol. 58, No. 12, 4033–4041, 2010.
22. Hojjati, A., M. Soleimani, V. Nayyeri, and O. M. Ramahi, "Ternary optimization for designing metasurfaces," *Scientific Reports*, Vol. 11, No. 1, 1–9, 2021.